

An optimization model for fragmentation-based routing in delay tolerant networks

Xuyan BAO*, Yong ZHANG, Da GUO & Mei SONG

School of Electronic Engineering, Beijing University of Posts and Telecommunications, Beijing 100876, China

Received June 15, 2015; accepted August 30, 2015; published online January 4, 2016

Abstract The explosive growth of mobile data traffic has raised big penetration to cellular network. Fortunately, offloading part of traffic through Delay Tolerant Network (DTN) would be a promising option to relieve load pressure. However, the existing routing strategies designed for DTNs are inappropriate in offloading scenario, where i) large data item would take on the dominance of mobile traffic, ii) centralized control can be exploited with merge between DTN and cellular network. To improve the routing performance of large data transmission, we propose a novel optimization model by creating two-tier solution space based on fragmentation, maximizing the probability that the requested data item is successfully delivered before expiration, taking limited buffer space as constraint metric. Moreover, a specific routing scheme is instantiated from our model, which is supported by uniform fragmentation and fine-grained path selection. Extensive trace-driven simulations show that our scheme is more appropriate for offloading case with outstanding performance in terms of replication overhead and acceptable routing capability.

Keywords multi-path routing, delay tolerant networks, optimization model, data offloading, stochastic orderings

Citation Bao X Y, Zhang Y, Guo D, et al. An optimization model for fragmentation-based routing in delay tolerant networks. *Sci China Inf Sci*, 2016, 59(2): 022314, doi: 10.1007/s11432-015-5501-9

1 Introduction

We envision a future in which an era of Big Data is promoted by the overwhelming growth trend of mobile data traffic. Cisco forecasts that global mobile data traffic will increase nearly 11-fold from 2013–2018 and reach over 15 exabytes per month in 2018 [1]. Such amount of data traffic will raise big penetration to the cellular networks. To relieve load pressure, some recent studies [2–4] have proposed to offload a portion of cellular traffic through Delay Tolerant Networks, where data is exchanged among mobile nodes by exploiting the opportunistic contacts. Meanwhile, there exists two salient features in offloading scenario: i) the routing performance in such heterogeneous environment can be assisted by the centralized scheduling of cellular networks, compared to the conventional distributed routing applied to DTNs; ii) multimedia content, e.g., video clips, high-quality music files, would take on the dominance of mobile data. This type of data is generally large in size and can be hardly transmitted over a single contact.

* Corresponding author (email: sdlbxy19890106@sina.com)

In this paper, our work is motivated by the following question: Combining the advantage of centralized control from cellular networks and the large-size property of mobile data traffic, can we design a generic optimization model that may induce the global optimal routing strategy? To address the problem mentioned above, we propose a novel optimization model to formulate large data routing. The ultimate goal is to fulfill each request as much as possible, which means the probability that data can be successfully delivered before expired time should be maximized. Methodologically, we abstract the model as an optimization problem, which comprises three key factors.

Solution space. Each request triggers a ‘many-to-one’ transmission, where ‘many’ and ‘one’ refer to the users that hold and subscribe the data respectively. To overcome the limited buffer space and contact duration, we split the raw data into several packets to exploit multi-path transmission, instead of unicast approach. In our model, we establish primary and secondary solution space based on binary-matrix, aiming at depicting the packet allocation for data holders and packet replication for delivery paths.

Objective function. The requested data can be delivered before expired time as long as the subscriber collects adequate number of packets to reconstruct the data. In our model, the objective function is represented as the product of the probability that each packet is successfully delivered. It is noteworthy that each term in the expression can be calculated through the delay distribution of opportunistic path (see Section 3), which is uniquely determined by the inter-contact time of node pairs within the path.

Constraints. Assume packet allocation and replication have been resolved, i.e., each packet is specifically assigned to some opportunistic paths. Then the whole multi-path transmission can be decomposed into several unicast routing, i.e., packets are transmitted along a single path. Some recent researches have investigated the impact of contact duration upon packet-level replication [5] and load allocation [6]. Thus in our model, we take the node buffer as the major constraints since the limited buffer space would affect the delay distributions of successive packets.

Summarizing, the major contributions of the paper are listed as follows:

- We propose a novel fragmentation-based optimization model to improve the routing performance of large data item applied to offloading scenario, which have two innovative parts: i) the design of two-tier solution space using binary matrix, ii) the analysis of packet delay using two-dimensional recursive formula under buffer constraint to determine the objective function.
- We provide a specific routing strategy derived from the aforementioned model, which have two desirable parts: i) the simplification of solution space based on uniform fragmentation, ii) the algorithm of path selection based on quasi stochastic orders.

The rest of the paper is organized as follows. Section 2 reviews the related work. Section 3 gives a detailed formulation of our optimization model. Section 4 instantiates a routing strategy derived from the above model. Section 5 evaluates the performance of the above strategy by trace-driven simulations. Section 6 concludes the paper.

2 Related work

On the one hand, due to the high mobility of DTNs, large data transfer hardly can be done within a single pairwise contact. Some coding techniques have been widely used to improve data transmission efficiency. Zhang et al. [7] show that the Random Linear Coding (RLC) for unicast in DTNs offers significant improvement. In a broader sense, Ref. [8] evaluated the performance of proactive and reactive fragmentation and Ref. [9] realized the lifetime maximization utilizing network coding. Although network coding and fragmentation are not the focus of this paper, it is evident that such perspective, that the raw data can be divided into a set of packets, is tenable at creating the solution space of our model.

On the other hand, using optimization method to formulate DTN problems have been studied in [10,11]. In [10], a cooperative cache-based content delivery framework is established based on the maximization of overall subscription served probability. In [11], the authors analyze the convergence conditions about whether the distributed sub-gradient method could lead to the optimal solution in DTN scenario. In fact, our model which benefits from centralized control may converge to the optimal solution, instead of

sub-optimal solution resulting from distributed approach.

Recently, a generic model named DTN-Meteo [12] is proposed to forecast the performance of a class of utility-based routing algorithms. Besides the above functionality, our model further tends to output routing instructions. Routing schemes for DTNs have been well-developed and categorized by two major classes. One class aims at approaching the performance of epidemic routing by exploiting the forwarding metric to control data replication [13–15]. Some typical examples like the efficient routing of Single-copy case and Multiple-copy case are investigated in [16, 17], resp. Another class revolves around the social relationships of mobile nodes to design routing strategy [18–20], in SimBet [21] and BUBBLE Rap [22], they all improve delivery performance based on social metrics such as centrality, betweenness, modularity, etc. Also, Ref. [23] propose a novel scheme for data forwarding by exploiting the transient social contact patterns.

To sum up, all the routing schemes mentioned above are mostly applied to DTN environment or processing the data item as integral, which means the routing procedure has to be conducted in a distributed manner and leads to incomplete data transmission. In this paper, we present a routing scheme utilizing multi-path transmission and global optimization to fulfill each data request to the uttermost.

3 Formulation

We consider a large data routing scenario over the N -node network, where data-transfer relies on intermittent multi-hop paths formed by a sequence of node contacts. The big picture of our model is shown in Figure 1, s denotes the node attached with data-request of finite expired time T_e , and the raw data is encoded into L packets, denoted by $c = \{c_1, c_2, \dots, c_L\}$. $V_h = \{h_1, h_2, \dots, h_\alpha\}$ denotes the node set including all the available data holders. For each holder h_i , there exists a Path-Set $P_{h_i \rightarrow s} = \{p_1, p_2, \dots, p_{n(h_i)}\}$ connecting s and h_i . Node contacts are represented by the network contact graph $G(V, E)$, where the contact process between a pair of nodes $i, j \in V$ is modeled as an edge $e_{ij} \in E$. The characteristics of an edge are determined by the pairwise intercontact time, which is distributed as a power law with an exponential cut-off [24]. Assume that each data request is randomly generated and initiates routing through a set of opportunistic paths. To proceed, we define the multi-hop opportunistic path on $G(V, E)$, as appeared in [25] with subtle modification.

Definition 1. Opportunistic path

A r -hop opportunistic path $P_{AB} = (V_p, E_p)$ between nodes A and B consists of a node set $V_p = \{A, N_1, N_2, \dots, N_{r-1}, B\} \subset V$ and an edge set $E_p = \{e_1, e_2, \dots, e_r\} \subset E$ with edge weights $\{\lambda_1, \lambda_2, \dots, \lambda_r\}$. Path weight $w_{AB}(T)$ is the probability that data is opportunistically transmitted from A to B along P_{AB} within time T .

As previously described, each edge e_k on P_{AB} is indeed bonded with a node-pair, this implies that the cumulative distribution function (CDF) of intercontact time J_k between nodes N_k and N_{k+1} can be used to measure the edge weight, i.e., λ_k . Particularly, we let the random variable J_k follow Pareto-Exponential distribution with probability density function (PDF):

$$p_{J_k}(x) = C_{ij} \cdot x^{-\alpha_{ij}} \cdot e^{-\beta_{ij}x} \cdot \left(\frac{\alpha_{ij}}{x} + \beta_{ij} \right), \quad (1)$$

where i, j denote the node pair joined by e_k . Eq. (1) can be derived from the complementary cumulative distribution function (CCDF) in [12]. Now, from Eq. (1), $\lambda_k (k \in [1, r])$ can be written as

$$\lambda_k(T) = \int_0^T p_{J_k}(x) dx. \quad (2)$$

To facilitate the calculation of path weight $w_{AB}(T)$ based on Eq. (2), we express the delay of a path with r -hops in a recursive form of

$$D_k = D_{k-1} + J_k, \quad 2 \leq k \leq r, \quad D_1 = J_1. \quad (3)$$

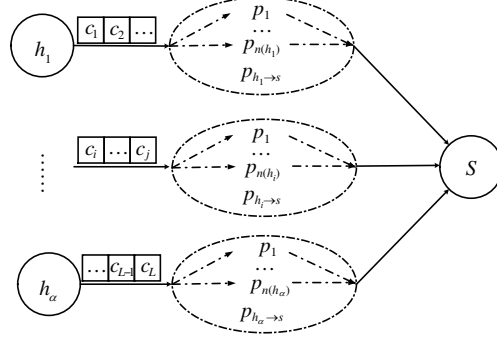


Figure 1 Fragmented multi-path routing.

Note that Eq. (3) implies the contact time is negligible to data transfer delay between any two nodes compared with intercontact time. Then, the path weight can be computed as follows:

$$\begin{aligned}
 w_{AB}(T) &= \Pr(D_r \leq T) \\
 &= \int \int_{D_{r-1} + J_r \leq T} p_{D_{r-1}}(x) \cdot p_{J_r}(y) dx dy \\
 &= \int_0^T w_{AN_{r-1}}(T - y) \cdot p_{J_r}(y) dy.
 \end{aligned} \tag{4}$$

Thus, Eq. (4) yields a practical way to calculate $w_{AB}(T)$ from initial condition $D_1 = J_1$ by convolutions. Next, we interpret the optimization model as a fragmentation problem formulated as follows:

Definition 2. the fragmentation problem is to determine the optimal solution $X = (\mathbf{x}^1, \mathbf{x}^2, \dots, \mathbf{x}^\alpha)$ which maximize the probability that data is successfully transferred within T_e through a path-set (PS), subject to a given buffer-constraint (BC).

$$\max \prod_{m=1}^L \Pr_{c_m \rightarrow s}^{T_e} \quad \text{s.t.} \quad \mathbf{b} \in \mathbb{R}^N. \tag{5}$$

3.1 Notations

(1) $X = (\mathbf{x}^1, \mathbf{x}^2, \dots, \mathbf{x}^\alpha)$ is First-Degree-Fragmented-Matrix (FDFM), resp. V_h . The column vector $\mathbf{x}^i (i \in [1, \alpha])$ with dimension L represents the allocation-solution of h_i , each component $x_j^i (j \in [1, L])$ of \mathbf{x}^i only takes 0 or 1, indicating whether packet c_j is assigned to h_i .

(2) $\mathbf{L}_p = (L_1, L_2, \dots, L_\alpha)$ is the packet-load vector, where each component denotes the amount of packets required to be offloaded by h_i . Specifically, we can obtain \mathbf{L}_p by adding all the row vectors of X .

(3) $F_i = (\mathbf{f}^1, \mathbf{f}^2, \dots, \mathbf{f}^{n(h_i)})$, $i \in [1, \alpha]$ is Second-Degree-Fragmented-Matrix (SDFM), resp. h_i . The column vector $\mathbf{f}^j (j \in [1, n(h_i)])$ with dimension L_i represents the allocation-solution of path $p_j \in P_{h_i \rightarrow s}$, each component $f_k^j (k \in [1, L_i])$ of \mathbf{f}^j only takes 0 or 1, indicating whether packet c_k is assigned to p_j .

(4) $\prod_{m=1}^L \Pr_{c_m \rightarrow s}^{T_e}$ is the probability that each packet is successfully transmitted from h_i to s within time T_e , i.e., the requested data can be reconstructed before time expires.

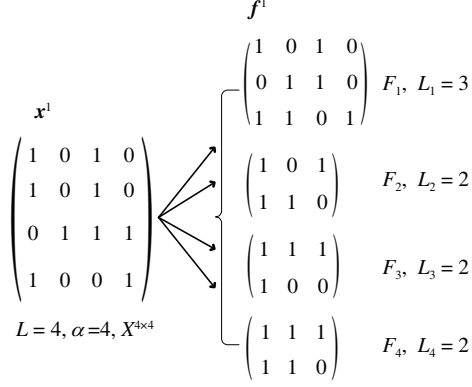
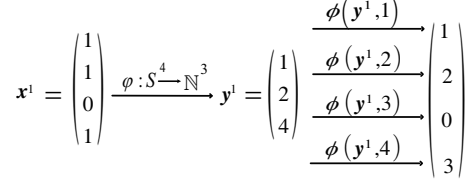
(5) Path-Set (PS) is the universal set including all the paths from $\{P_{h_1 \rightarrow s}, P_{h_2 \rightarrow s}, \dots, P_{h_\alpha \rightarrow s}\}$, $|PS| = \sum_{i=1}^\alpha n(h_i)$.

(6) Buffer-Constraint (BC) is a real vector, denoted by \mathbf{b} , each component $b_i (i \in [1, N])$ indicates the buffer space of node V_i .

Based on the above notations, we illustrate how to derive the analytical expression of $\prod_{m=1}^L \Pr_{c_m \rightarrow s}^{T_e}$ to make the above formulation explicit.

3.2 Solution space

First, given one feasible solution X , we extract \mathbf{L}_p from X to control the dimension of column vectors belonging to matrix F_i . Indeed, this approach can be interpreted as decomposing the solution space into


Figure 2 Extraction from FDFM to SDFM.

Figure 3 Mapping from FDFM to SDFM.

equivalent sub ones. Thus, each F_i appears in the form of undetermined matrix to provide feasible domain of path-allocation with respect to each h_i . Furthermore, we define a compound mapping to establish the connections between the FDFM and the SDFM.

Definition 3. Let $a(p, q)$ be the statement: x_p^i is the q th component that equals to 1. Define $\varphi: S^\delta \rightarrow \mathbb{N}^\varepsilon$, $\phi: \mathbb{N}^\varepsilon \times \mathbb{N} \rightarrow \mathbb{N}$ by

$$\begin{aligned} \mathbf{y}^i &= \varphi(\mathbf{x}^i) \text{ i.e. } y_q^i = p, \text{ iff, } (x_p^i = 1 \wedge a(p, q))|_{p=1,2,\dots,\delta}, \\ z &= \phi(\mathbf{y}^i, k) \text{ i.e. } z = q, \text{ if, } y_q^i = k, \text{ otherwise, } z = 0, \\ q &= 1, 2, \dots, \varepsilon, \quad k = 1, 2, \dots, \delta, \\ \text{where } S &= \{0, 1\}, \mathbb{N} = \{1, 2, \dots, L\}, 1 \leq \varepsilon \leq \delta \leq L. \end{aligned}$$

As illustrated in Figure 2, c_1, c_2, c_4 would be assigned to holder h_1 , determined by the first column vector \mathbf{x}^1 . After extracting F_1 from X , let $\delta = L = 4$, $\varepsilon = L_i = 3$, we establish a one-to-one mapping between \mathbf{x}^1 and the packet index of F_1 as shown in Figure 3. we say packets (1,3) of F_1 are assigned to path p_1 of h_1 , indeed, pointing to c_1, c_4 . To calculate the delivery delay of each packet, let $\delta = L_i, i \in [1, \alpha]$, $\varepsilon = \sum_{k=1}^{L_i} f_k^j, j \in [1, n(h_i)]$, we further establish the similar mapping structures between SDFM and the packet index of each specific path.

3.3 Objective function and constraints

Second, a crucial point that arises with the explicit expression (Eq. (2)) of path weight is the footstone to determine the objective probability function. Hereafter, we assume exact one packet can be transferred during a contact. This assumption has been solidly made in [2] and provides sufficient analytical insights in general cases.

Generally, once FDFM and SDFM are determined, for any opportunistic path, a First-In-First-Out (FIFO) packet queue with length $\sum_{k=1}^{L_i} f_k^j$ is instantiated, then it is fairly to conclude the probability that the first packet is successfully delivered to s within T_e is just the path weight at time T_e , i.e., $w_{p_j, s}(T_e)$. Nonetheless, the delivery delay of the following packets is mutually dependent, In the following, we use 2-dimensional recursive formula to analyze the delivery delay of each packet transmitted by path p_j with R hops. The inspiration behind this methodology is originated from the dependence of successive packets. Specifically, let $d(l, r), 1 \leq l \leq \sum_{k=1}^{L_i} f_k^j, 1 \leq r \leq R$ denote the r -hop delay of the l -th packet from node r to $r+1$, then, the distribution of delivery delay of the l -th packet, i.e., $d_l = \sum_{r=1}^R d(l, r)$, can be indirectly derived by defining the following events (as shown in Figure 4):

Event A. The $(l+1)$ -th packet is transferred from node h_i to node k .

Event B. The l -th packet is transferred from node h_i to node $k+1$.

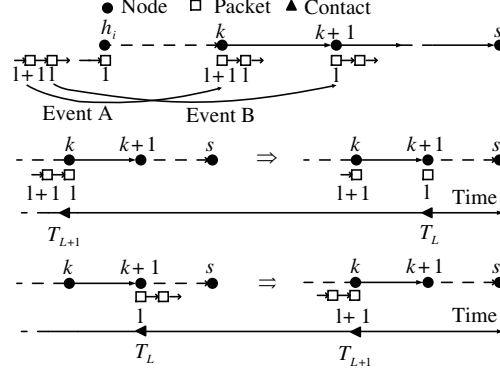


Figure 4 Packet block between successive node-pair.

Let $T^{(l+1)}$, $T^{(l)}$ be the time elapsed when event A, B happens, respectively. Then, we have

$$T^{(l+1)} = \sum_{r=1}^{k-1} d(l+1, r), \quad T^{(l)} = \sum_{r=1}^k d(l, r). \quad (6)$$

(a) $T^{(l+1)} < T^{(l)}$, which means when the $(l+1)$ -th packet arrives at node k , the l -th packet still resides in node k and will stay for another $T^{(l)} - T^{(l+1)}$ time interval to leave for node $k+1$, after that, since the contacts between node k and $k+1$ form a renewal process, only after J_k time is the transfer of the $(l+1)$ -th packet achieved from node k to $k+1$. Thus, we can derive the recursive form of $d(l+1, k)$ as follows:

$$d(l+1, k) = J_k + (T^{(l)} - T^{(l+1)}). \quad (7)$$

(b) $T^{(l+1)} > T^{(l)}$, which means when the $(l+1)$ -th packet arrives at node k , the l -th packet has departed from node k to $k+1$ for $T^{(l+1)} - T^{(l)}$ time interval, so the residual time for the $(l+1)$ -th packet to wait for the next contact opportunity is

$$d(l+1, k) = J_k - (T^{(l+1)} - T^{(l)}). \quad (8)$$

With initial condition: $d(1, k) = J_k, 1 \leq k \leq R$.

However, the limited buffer space of intermediate nodes may introduce the extra delay, say $\tilde{d}(l, r)$, into $d(l, r)$. Assume the l -th packet is carried by V_r and about to be transferred to V_{r+1} when a contact arises, but the buffer of V_{r+1} is full, which means the l -th packet would be rejected by V_{r+1} and ‘back-off’, waiting for the next contact opportunity. Let $J_{r,1}, J_{r,2}, \dots, J_{r,\infty}$ be a sequence of independent identically distributed random variables which obeys the distribution of J_r , then the probability that the l -th packet is back-off for n times is

$$P_n \left[\tilde{d}(l, r) = \sum_{i=1}^n J_{r,i} \right] = \left(\frac{1}{b_{r+1}} \right)^n \left(1 - \frac{1}{b_{r+1}} \right). \quad (9)$$

Now, let $E[J_r] = \mu_r$, the expectation of $\tilde{d}(l, r)$ conditioning on n can be expressed as

$$E[\tilde{d}(l, r)] = \sum_{i=1}^{\infty} E[\tilde{d}(l, r) | n = i] P\{n = i\} = \sum_{i=1}^{\infty} i \mu_r \cdot \left(\frac{1}{b_{r+1}} \right)^i \left(1 - \frac{1}{b_{r+1}} \right) = \frac{\mu_r}{b_{r+1} - 1}. \quad (10)$$

Taking $E[\tilde{d}(l, r)]$ as additive term into Eq. (6), combined with Eqs. (7) and (8), $d(l+1, k)$ is rewritten as

$$d(l+1, k) = J_k + \sum_{r=1}^k d(l, r) - \sum_{r=1}^{k-1} d(l+1, r) + \frac{\mu_k}{b_{k+1} - 1}. \quad (11)$$

Consequently, no matter which event happens first, Eqs. (7) and (8) are identical in the final expression. The k -hop delay of the $(l+1)$ -th packet depends on not only the delivery delay of the l -th packet from V_1

to V_{k+1} but also the delivery delay of the $(l+1)$ -th packet from V_1 to V_k . Finally, to facilitate the explicit expression of the objective function, we define the indicator function as follows:

$$I_{ij}(k) = \begin{cases} 1, & \text{if } (x_k^i = 1) \wedge (f_t^j = 1), t = \phi(\varphi(\mathbf{x}^i), k), \\ 0, & \text{otherwise.} \end{cases} \quad (12)$$

Eq. (12) represents that if packet k is not only assigned to the data holder h_i but also transferred by path p_j belonging to h_i , then $I_{ij}(k)$ is set to 1, otherwise 0. By combining the set of the delay distributions, the compound mappings and the indicator function, the objective function can be calculated in the form of

$$\prod_{m=1}^L \Pr_{c_m \rightarrow s}^{T_e} = \prod_{m=1}^L \left\{ 1 - \left[\prod_{i=1}^{\alpha} \prod_{j=1}^{n(h_i)} I_{ij}(m) \cdot \Pr(d_l > T_e) \right] \right\}, \quad (13)$$

$$l = \phi\{\varphi(\mathbf{f}^j), \phi[\varphi(\mathbf{x}^i), m]\}.$$

Theoretically, any type of fragmentation-based routing strategy can be interpreted as decomposing the raw data into a number of packets and utilizing parallel transmission. It follows that the raw data can be reconstructed as long as the requester collects adequate packets. This explains the multiplicative relationships of each term $\Pr_{c_m \rightarrow s}^{T_e}$, which represents the probability that packet m can be delivered before expiration. Since a packet eventually would be assigned to a specific path, expressed by the compound mapping l within Eq. (13), of solution space, this tight connection implies that whether a packet is delivered before T_e is up to the delay distribution of a specific path it relies on. It is the probability term that can be calculated as ‘1-the probability that the delay of each packet m exceeds the expired time T_e ’. Due to the complexity of our model, a novel routing scheme is derived by simplified handling in the next section.

4 Instantiation

When a data request is generated, the consequent routing instructions would be determined by solving the fragmentation problem (Definition 2). It is necessary to outline the big picture so as to fit in the practical scenario. First, a contact would be recorded when a terminal detects adjacent peers, we set up a warm-up period for the network operator to collect nodes’ statistical information, including contact times and occupied buffer condition. Second, we adopt a parameter estimation method (e.g., Maximum Likelihood Estimation, MLE) to determine the distribution of intercontact time catering for the calculation of path delay. Last, we use encoding techniques (e.g., Random Linear Network Coding) to split the raw data into several packets and allocate them based on FDFM and SDFM.

It is impractical to optimize traversing the whole two-tier solution space, however each term of Eq. (5) can be computed if only FDFM and SDFM are settled, turning into the following issues: 1) How to allocate the packets for holders to ascertain the FDFM? 2) How to allocate the packets for delivery paths to ascertain the SDFM?

4.1 Simplification of solution space

The initial design of FDFM implies that the packet heterogeneity, including packet size, redundancy degree, etc., is intrinsically combined with our model, which means different packets make various contribution to the final reconstruction. We create an enormous solution space in exchange for universality, which yields the intractability of approaching optimality. Hence, we fragment the raw data in identical size to compress the space of FDFM, represented as a ‘‘packet-ring’’.

The variable parts of original solution space would be reduced to [start-packet-index, finish-packet-index], we use a $2 \times \alpha$ matrix to denote the simplified FDFM as follows:

$$\mathbf{x}^i = (s_i, t_i)^T, i \in [1, \alpha] \Rightarrow X^{2 \times \alpha} = \begin{pmatrix} s_1 & \cdots & s_\alpha \\ t_1 & \cdots & t_\alpha \end{pmatrix}. \quad (14)$$

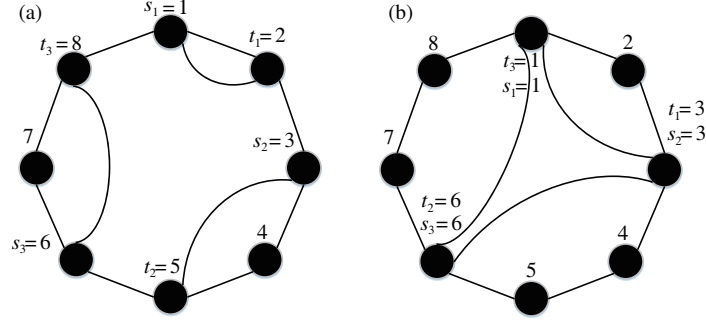


Figure 5 Packet-load allocation. (a) Minimal allocation; (b) extended allocation.

Each packet with identical size erases the impact from the order change of packet index, e.g., assume two holders have the requested data fragmented into five packets. let $\mathbf{a} = (1, 0, 1, 0, 1)^T$, $\mathbf{b} = (0, 1, 0, 1, 0)^T$, $\mathbf{c} = (1, 1, 1, 0, 0)^T$, $\mathbf{d} = (0, 0, 0, 1, 1)^T$, then (\mathbf{a}, \mathbf{b}) and (\mathbf{c}, \mathbf{d}) indeed yield the same results when calculating the objective function. Thus, we regulate $(s_i, t_i)^T$ provides a continuous pattern, e.g., $(1, 4)^T$ means c_1, c_2, c_3, c_4 are allocated to h_i , the packet-load L_i becomes

$$L_i = \begin{cases} t_i - s_i + 1, & t_i > s_i, \\ t_i + L - s_i + 1, & t_i < s_i. \end{cases} \quad (15)$$

Overlapping is viable since any packet can be allocated to multi-holders. It is the length of overlapping parts that is utilized to traverse over $X^{2 \times \alpha}$. Now, we propose a search algorithm including three factors: initial point, iterative step, iterative direction.

Whether the raw data can be reconstructed before expiration or not is depending on the packet with the largest delivery delay, which is analogous to the ‘‘Cask Effect’’. To balance delay difference, we take inverse proportional relation to control the packet-load between holders.

$$\frac{1}{L_i} \propto E(p_i), \quad (16)$$

where p_i is the path which has the minimum expected delay $E(p_i)$ from h_i to s . Given the following inequality:

$$L \leq L_1 + L_2 + \cdots + L_\alpha \leq L \cdot \alpha. \quad (17)$$

Indeed, the sum of packet-load must be larger than L such that the raw data can be reconstructed. Combining with Eq. (16), the initial point is determined by $\sum_{i=1}^{\alpha} L_i = L$, which yields the minimal packet allocation without overlapping part. Note that either s_i or t_i only takes integer, which implies the feasible domain is the proper subset of $[L, L \cdot \alpha]$. Thus, We set up the iterative step, denoted by τ , as a positive integer to control the iterative precision. Suppose $\tau = 1$, a packet-ring with 8 packets, and 3 holders. Based on Figure 5(a) which shows the minimal packet allocation, we fix s_i , then extend t_i with τ packets to generate a new feasible solution, as shown in Figure 5(b).

In fact, two directions are available to be chosen as iterative direction. CW: fix s_i , extend t_i with τ_i packets clockwise, e.g., if we fix s_1 , extend t_1 with τ_1 packets.

$$X_{cw} = \begin{pmatrix} s_1 & \cdots & s_\alpha \\ (t_1 + \tau_1) \bmod L & \cdots & (t_\alpha + \tau_\alpha) \bmod L \end{pmatrix}. \quad (18)$$

CCW: fix t_i , extend s_i with τ_i packets counterclockwise, e.g., if we fix t_1 , extend s_1 with τ_1 packets.

$$X_{ccw} = \begin{pmatrix} (s_1 - \tau_1) \bmod L & \cdots & (s_\alpha - \tau_\alpha) \bmod L \\ t_1 & \cdots & t_\alpha \end{pmatrix}. \quad (19)$$

In Eqs. (18) and (19), any τ_i can be determined by τ_1 , Eqs. (15) and (16). Actually, we only need either choose CW or CCW, which yields the same result due to the irrelevance of packet index.

4.2 Path selection

In our model, the objective function is composed of probabilistic terms, each of which relies on the delay distribution of opportunistic paths. To maximize Eq. (5), the most intuitive approach is to find the path which yields the minimum value of $\Pr(d_l > T_e)$. Above motivates us by a fundamental question: Is there a primitive stochastic order to compare the delivery delay of opportunistic paths? To proceed, we need the following definition and equivalent conditions for the stochastic orderings.

Definition 4 ([26]). X is said to be smaller than Y in the usual stochastic order (denoted by $X \leq_{st} Y$) if $E[\phi(X)] \leq E[\phi(Y)]$ holds for all increasing functions ϕ for which the expectations exist, or equivalently if $P\{X > u\} \leq P\{Y > u\}$ for all $u \in (-\infty, +\infty)$.

If $X \leq_{st} Y$, then $P\{X > T_e\} \leq P\{Y > T_e\}$ by taking $u = T_e$. Also, we have $E(X) \leq E(Y)$ by taking $\phi(t) = t$. It follows that Definition 4 provides us a strict condition to compare random variables. Ref. [27] reveals that replicating packets along a small number of paths suffice to capture most of the achievable gain with respect to delivery delay. To control the solution space of SDFM, we restrict the replication limit as 2. Next, we stochastically compare the delay performance of two-hop opportunistic paths connecting s and h_i , which yields sufficient analytical insights and forms the basis for extended evaluation of multi-hop paths.

Let Z_1, Z_2 be the delivery delays of two 2-hop paths, and r_1, r_2 be the relay nodes. X_1, Y_1, X_2, Y_2 represent the intercontact time between node pairs $(s, r_1), (r_1, h_i), (s, r_2), (r_2, h_i)$, respectively. Then, we have

$$\begin{cases} Z_1 = X_1 + Y_1, \\ Z_2 = X_2 + Y_2. \end{cases} \tag{20}$$

To facilitate the calculation of Eq. (20), we denote the CCDF, CDF, PDF by $\bar{F}(\cdot), F(\cdot), p(\cdot)$, respectively. Rewrite Eq.(1)

$$p_{ij}(x) = C_{ij}(\alpha_{ij} \cdot x^{-\alpha_{ij}-1} + \beta_{ij} \cdot x^{-\alpha_{ij}}) \cdot e^{-\beta_{ij}x}, \tag{21}$$

where $C_{ij} = (t_{ij})^{\alpha_{ij}} \cdot e^{\beta_{ij}t_{ij}}$ is determined by the minimum intercontact time t_{ij} , $i, j \in \{1, 2\}$ denote the i -th path and the j -th hop, accordingly. Next, we compute the CCDF of Z_1 as follows:

$$\begin{aligned} \bar{F}(z_1) &= P\{X_1 + Y_1 > z_1\} \\ &= \int_{0^+}^{+\infty} \left(\int_{z_1-y_1}^{+\infty} p_{11}(x_1)dx_1 \right) \cdot p_{12}(y_1)dy_1. \end{aligned} \tag{22}$$

Due to the various t_{ij} of different node pairs, Eq.(22) can be further developed as

$$\bar{F}(z_1) = \int_{t_{12}}^{+\infty} \bar{F}_{11}(z_1 - y_1) \cdot p_{12}(y_1)dy_1. \tag{23}$$

The form of CCDF is shown in [12],

$$\bar{F}_{ij}(x) = \begin{cases} C_{ij} \cdot x^{-\alpha_{ij}} \cdot e^{-\beta_{ij}x}, & x \geq t_{ij}, \\ 1, & 0 < x < t_{ij}. \end{cases} \tag{24}$$

Combining Eqs. (21), (24), and (23) is intrinsically embedded with piecewise property if we integrate from t_{12} to $+\infty$ with respect to y_1 . If $z_1 < t_{11} + t_{12}$, then $\bar{F}(z_1) = 1$; otherwise

$$\begin{aligned} \bar{F}(z_1) &= \int_{t_{12}}^{z_1-t_{11}} C_{11}(z_1 - y_1)^{-\alpha_{11}} e^{-\beta_{11}(z_1-y_1)} \cdot p_{12}(y_1)dy_1 + \int_{z_1-t_{11}}^{+\infty} p_{12}(y_1)dy_1 \\ &= C_{11}C_{12}z_1^{-\alpha_{11}} e^{-\beta_{11}z_1} \cdot \int_{t_{12}}^{z_1-t_{11}} f(y_1)dy_1 + \bar{F}_{12}(z_1 - t_{11}), \\ f(y_1) &= \left(1 - \frac{y_1}{z_1}\right)^{-\alpha_{11}} \cdot (\alpha_{12} \cdot y_1^{-\alpha_{12}-1} + \beta_{12} \cdot y_1^{-\alpha_{12}}) \cdot e^{(\beta_{11}-\beta_{12})y_1}. \end{aligned} \tag{25}$$

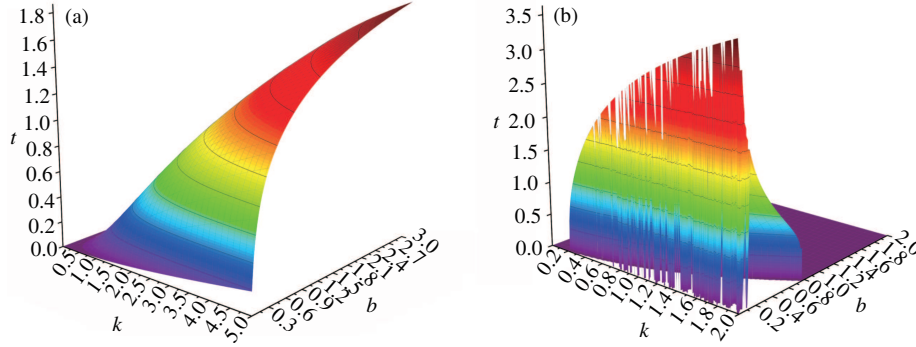


Figure 6 Distribution surface of t . (a) Surface under $a=0.5$; (b) surface under $a=-0.5$.

In Eq. (25), we expand the term $\left(\frac{1}{1-y_1/z_1}\right)^{\alpha_{11}}$ by Newton's Generalized Binomial Theorem:

$$\left(\frac{1}{1-y_1/z_1}\right)^{\alpha_{11}} = \sum_{k=0}^{\infty} C_{\alpha_{11}+k-1}^k \left(\frac{y_1}{z_1}\right)^k, \quad (26)$$

where $C_{\alpha_{11}+k-1}^k = \alpha_{11}(\alpha_{11}+1)\cdots(\alpha_{11}+k-1)/k!$. Substituting the corresponding term in Eq. (25) with Eq. (26), if $\beta_{11} < \beta_{12}$, we obtain

$$\bar{F}(z_1) = K_1 \cdot z_1^{-\alpha_{11}} e^{-\beta_{11}z_1} + \bar{F}_{12}(z_1 - t_{11}) + o(z_1^{-\alpha_{11}} e^{-\beta_{11}z_1}), \quad (27)$$

where K_1 is a constant and $o(\cdot)$ is the higher-order infinitesimal of (\cdot) (see Supporting information for details). Similarly, assume $\beta_{21} < \beta_{22}$, the CCDF of Z_2 is given by

$$\bar{F}(z_2) = K_2 \cdot z_2^{-\alpha_{21}} e^{-\beta_{21}z_2} + \bar{F}_{22}(z_2 - t_{21}) + o(z_2^{-\alpha_{21}} e^{-\beta_{21}z_2}). \quad (28)$$

From Eqs. (27) and (28), omitting the higher-order infinitesimals, the CCDF of two-hop delay can be approximately represented as a linear combination of the CCDFs of constituent single-hop delay. To proceed, taking $f_1(x) = C_{11} \cdot x^{-\alpha_{11}} e^{-\beta_{11}x}$, $f_2(x) = C_{21} \cdot x^{-\alpha_{21}} e^{-\beta_{21}x}$, we compare $f_1(x)$ and $f_2(x)$ by determining the X-coordinate of intersection point:

$$f_1(x) = f_2(x) \Rightarrow C_{11}/C_{21} = x^{\alpha_{11}-\alpha_{21}} \cdot e^{(\beta_{11}-\beta_{21})x}. \quad (29)$$

Let $C_{11}/C_{21} = K$, $\alpha_{11} - \alpha_{21} = a$, $\beta_{11} - \beta_{21} = b$, we obtain

$$K = x^a \cdot e^{bx} \xrightarrow{t=bx} K \cdot b^a \cdot t^{-a} = e^t. \quad (30)$$

Iterative approach can be adopted to solve Eq. (30) which is a transcendental equation in the form of numerical solution. Without loss of generality, assume $\beta_{11} > \beta_{21}$, which means the decreasing rate of f_1 is larger than that of f_2 , then $b \in (0, +\infty)$; moreover, C_{11} and C_{21} are positive constants, then $K \in (0, +\infty)$; Ref. [28] has revealed that the power index extracted from real traces is smaller than 1, then $|a| < 1$. Particularly, if we take $a = 0$, Eq. (30) would be reduced to $x = \ln(K)/b$, i.e., x is logarithmic to K and inverse proportional to b . In addition, two surfaces are shown in Figure 6 to depict the distribution of t under $a = 0.5$ and $a = -0.5$.

Based on Figure 6, we fix b and K to acquire intersection lines of ' t vs. K ' and ' t vs. b ' with the surface. By means of non-linear fitting, the following conclusions can be inferred from our numerical analysis: i) when $0 < \alpha_{11} - \alpha_{21} < 1$, there exists only one intersection point. If we recover the original variable using $t = bx_0$, then x_0 is increasing logarithmically as $K \rightarrow \infty$ while decreasing at approximate rate of $\ln(b)/b$ as $b \rightarrow \infty$; ii) when $-1 < \alpha_{11} - \alpha_{21} < 0$, if b is taken too large, which extremely compresses the shape of t^{-a} and yields no solution, otherwise, there maybe exists one or two intersection points. In the latter case, the smaller $t \ll 1$ incurs $x_0 = t/b$ is far less than t_{11} and t_{21} , i.e., $f_1(x_0) = f_2(x_0) = 1$. Such trivial solution can be excluded in comparing CCDF curves, while larger t is selected. Similarly,

x_0 is increasing logarithmically as $K \rightarrow \infty$ while decreasing at power rate less than 1 as $b \rightarrow \infty$. It is evident that the X-coordinate of f_1 and f_2 moves rather slowly along the X-axis no matter how K , a and b varies. Meanwhile, the following inequalities hold

$$\begin{cases} f_1(x) \geq f_2(x), & 0 < x \leq x_0, \\ f_1(x) < f_2(x), & x > x_0. \end{cases} \quad (31)$$

Inspired from (31), relaxing the strict conditions in Definition 4, we propose the following definition of quasi stochastic order.

Definition 5. Let D_1, D_2 be the delivery delay of two different multi-hop opportunistic paths, t_1, t_2 be the corresponding minimum delay. If $\exists x_0 > \max(t_1, t_2)$ s.t. $P\{D_1 > x_0\} = P\{D_2 > x_0\}$, then

- D_1 is said to be smaller than D_2 in the weak quasi stochastic order iff $\exists u \in (x_0, +\infty)$ s.t. $P\{D_1 > u\} \leq P\{D_2 > u\}$, denoted by $X_1 \leq_{wq} X_2$.

- D_1 is said to be smaller than D_2 in the strong quasi stochastic order iff $\int_{0+}^{\infty} P\{D_1 > u\}du \leq \int_{0+}^{\infty} P\{D_2 > u\}du$, denoted by $X_1 \leq_{sq} X_2$.

Suppose $D_1 = \sum_{i=1}^n X_i$ and $D_2 = \sum_{i=1}^m Y_i$, recall from the derivation of Eq.(27), we infer that $\bar{F}(D_1) \doteq \sum_{i=1}^n \alpha_i \bar{F}(x_i)$ and $\bar{F}(D_2) \doteq \sum_{i=1}^m \beta_i \bar{F}(y_i)$. Thoroughly, the weak and strong quasi stochastic order provide qualitative and quantitative comparisons respectively. The weak orderings are based on partial comparison only defined over $[x_0, +\infty)$. Luckily, the expired time is commonly set as $T_e \gg x_0$ in offloading scenario, which means $\Pr(d_l > T_e)$ can be used as metric to evaluate weak orderings and optimize the objective function. While strong orderings give a comparison by quantifying the distance between CCDFs, which is equivalent to the second order stochastic dominance. However, if the optimal path is determined by strong orderings, congestion will arise due to the merge of traffic flow. While the weak orderings may yield different paths based on different T_e , which balances the network load.

5 Performance evaluation

In this section, we implement and evaluate the performance of our induced routing strategy named Optimal compared with the following schemes:

- Epidemic routing. The most generic routing based in DTNs that a node replicates the data to every encountered nodes that have not received a copy yet.
- Spray-and-Wait. A controlled-replication scheme that any node with $n > 1$ copies will forward $\lfloor n/2 \rfloor$ copies to the encountered node with no copy. The node with only one copy turns to direct transmission.
- Prophet [13]. An utility-based scheme that when a contact occurs, data is transferred from one node to another which owns the higher delivery predictability.
- RAPID [14]. An utility-driven scheme that treats DTN routing as a resource allocation issue, which is similar to our design concept. RAPID is composed of three parts: a selection algorithm, an inference algorithm and a control channel.

The number of copies L for each packet is initially set as 10% of all nodes N , which is applied to Spray-and-Wait and Prophet. For RAPID, we choose the average delay of packets as metric, upon each contact, RAPID replicates packets in decreasing order of marginal utility. The following metrics are used for evaluation:

- **Delivery ratio.** The ratio of data requests being fulfilled before expired time.
- **Delivery delay.** The average time a node takes to obtain the complete data after throwing a data request.
- **Replication overhead.** The number of data copies generated in the network.

5.1 Simulation setup

Our simulation is conducted on Matlab platform using cabspotting trace from the taxicabs of the city San Francisco, consisting of 536 taxis. The data record the GPS coordinates of each taxi which is equipped

with a GPS device collected over 30 days in the San Francisco Bay Area. The GPS sends the location information including time-stamps and Geo-coordinates periodically to the central server. Taking 1 min as the least time unit and calculating the distance between any node-pair, we make assumptions that nodes are in contact when their distance is less than the transmission range and define the inter-contact time as the time elapsing between two consecutive contacts. In experiment, 1 min is set as the driven time-slot with regard to the scale and contact density of traces. The first half of time-line is the training period for extracting all pairwise contact parameters C_{ij} , α_{ij} and β_{ij} by means of least square estimation, and the rest are reserved for data request and response.

5.1.1 Data generation

We generate 50 data items, each of which is uniformly fragmented into m packets, where m and packet-size are randomly selected within the range of $[4, 12]$ and $[0.5s, 1.5s]$ Mb, respectively. Thus, the data-size can be indirectly controlled by the adjustable parameter s . In initial phase, each data object is allocated to N th nodes called holders, where N th is uniformly distributed within $[1, 10\%N]$. Similarly, buffer space of nodes are uniformly distributed within $[200, 600]$ Mb.

5.1.2 Data request

Each node independently generates data request attached with a finite expired time $T_e \in [0.5T, 1.5T]$. Such process is implemented as a Poisson process which means the intercontact time between successive requests follows exponential distribution. In addition, we assume that request pattern follows Zipf distribution with default skewness parameter $w = 1.5$, particularly, let M be the number of data items, we have the probability that a request is generated for data j is $P_j = \frac{1}{j^w} / (\sum_{i=1}^M \frac{1}{i^w})$. It is noteworthy that when the time span of real trace is large, we need to increase the expired time accordingly by controlling T , which guarantees the comparison results will substantially hold.

5.2 Simulation results

5.2.1 Impact of average expired time

The simulation results with different value of T are shown in Figure 7. Optimal is slightly inferior to the rest of schemes in terms of delivery delay and ratio. In Figure 7(a), when expired time increases, the delivery delay of all schemes significantly rises, because more data lifetime leads to network congestion due to the limited buffer space. The performance of Epidemic, Spray-and-Wait, Prophet are nearly the same, since the contact density of cabspotting trace is adequate for transmission, while diminishes the delay improvement by replication. The reason why RAPID slightly outperforms these schemes is that the utility metric reflects not only the delivery delay but also the creation time, which means the aged packets are prioritized to replicate and deliver before expiration. However, Optimal is 7.2% (about 5 min) worse than that of other schemes. This is mainly due to the fixed routing path attached to each packet, which deteriorates the performance with wasting contact opportunity.

Figure 7(b) shows that the delivery ratio is improved as T increases, because packet has more time to be delivered before expiration. Optimal achieves a lower delivery ratio than that of other schemes from 6.2% to 1.5%. We infer that the threshold of path number, which still achieves profitable replication gain, implicitly results in degradation of delivery ratio due to insufficient exploration of extra paths. Also, as shown in Figure 7(c), Epidemic undoubtedly produces the maximum packet copies, followed by RAPID, Spray-and-Wait, Prophet. Comparatively, Optimal yields smaller number of copies than that of Prophet by 59%, Spray-and-Wait by 70.3%, RAPID by 105.8%, Epidemic by 138.8%. Summarizing, in offloading scenario, users who select DTNs to access data are usually delay-insensitive, which means 5 min (the worst case) is tolerable. Due to the limited resources of users, congestion caused by excessive data packets would impair network performance and consume nodes' buffer space swiftly. Therefore, Optimal which provides astonishing performance in terms of replication overhead still keeps acceptable routing capability, is more suitable for offloading case.

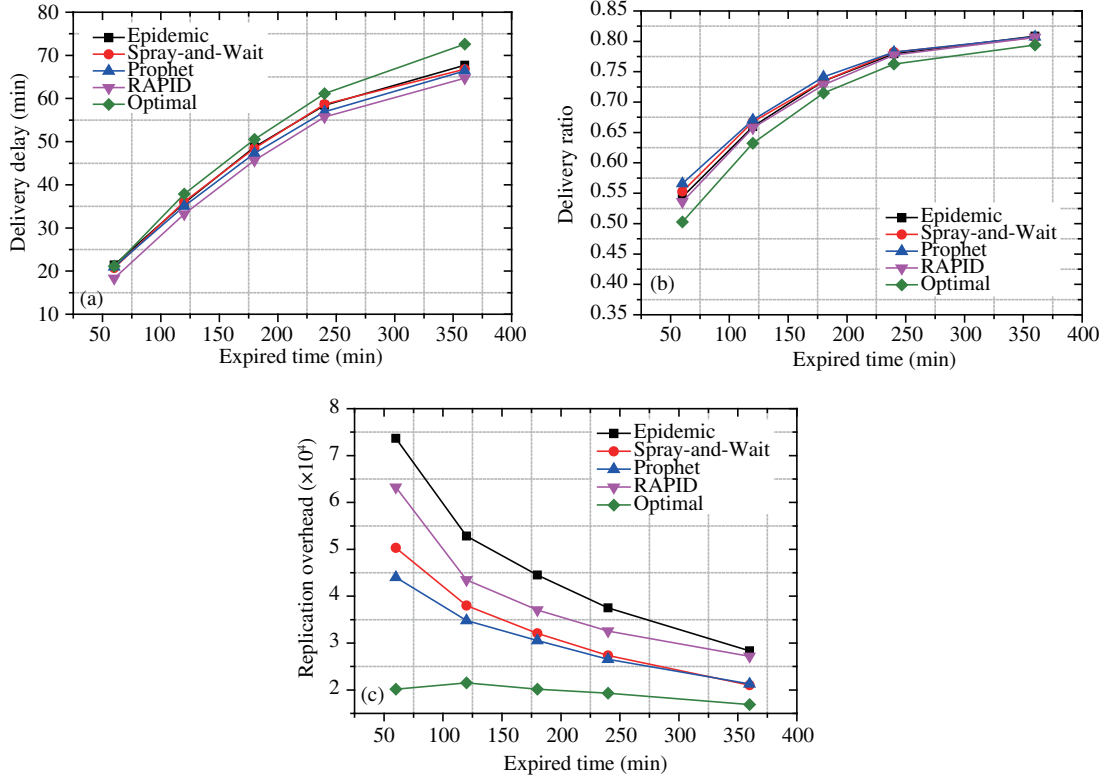


Figure 7 (Color online) Performance of data routing with different expired time. (a) Delivery delay; (b) delivery ratio; (c) replication overhead.

5.2.2 Impact of average packet size

The simulation results with different value of packet size are shown in Figure 8. As shown in Figure 8(a), RAPID outperforms and approaches Epidemic, Spray-and-Wait, and Prophet as packet size increases. In our settings, each data item is divided into several packets, hence we use packet size to control data size. If we speculate from another angle, given size of a data item, changing packet size identically means changing fragmented granularity. In Figure 8(a), the performances of all schemes except Optimal are distinguishable only when fine-grained fragmentation is adopted. In contrast, Optimal yields slightly longer delivery delay than that of Spray-and-Wait by 7.0%, Epidemic by 7.2%, Prophet by 7.4%, RAPID by 9.6% (about 3.3 min), but appears more non-volatile to various granularity. Also, Figure 8(b) reveals the degradation of all the schemes except Optimal since large packets consume buffer space. Similarly, Optimal is more stable and yields smaller delivery ratio than that of Prophet by 6.4%, Spray-and-Wait by 6.0%, Epidemic by 5.7%, RAPID by 5.7%.

The major advantage of Optimal is shown in Figure 8(c). As packet size increases, replication would be inhibited as large packets fill nodes' buffer up, which means the number of copies is decreasing. However, RAPID still produces amounts of copies when packet size is large, because the deletion of packet with minimal marginal utility relieves some buffer space. Additionally, Optimal yields smaller number of copies than that of Epidemic by 106%, RAPID by 226%, Spray-and-Wait by 77.2%, Prophet by 42.9%. To sum up, Optimal is more stable when fragmentation is adopted and still provides outstanding performance in terms of replication overhead.

5.2.3 Impact of initial number of holders

The simulation results with different value of initial holder number which represents data distribution density are shown in Figure 9. As shown in Figure 9(a), as holder number increases, the delay performance of all schemes except Optimal is significantly improved, since data is easier to be accessed by neighbor nodes. Meanwhile, high density of data coverage (above 10%) eliminates the performance gaps

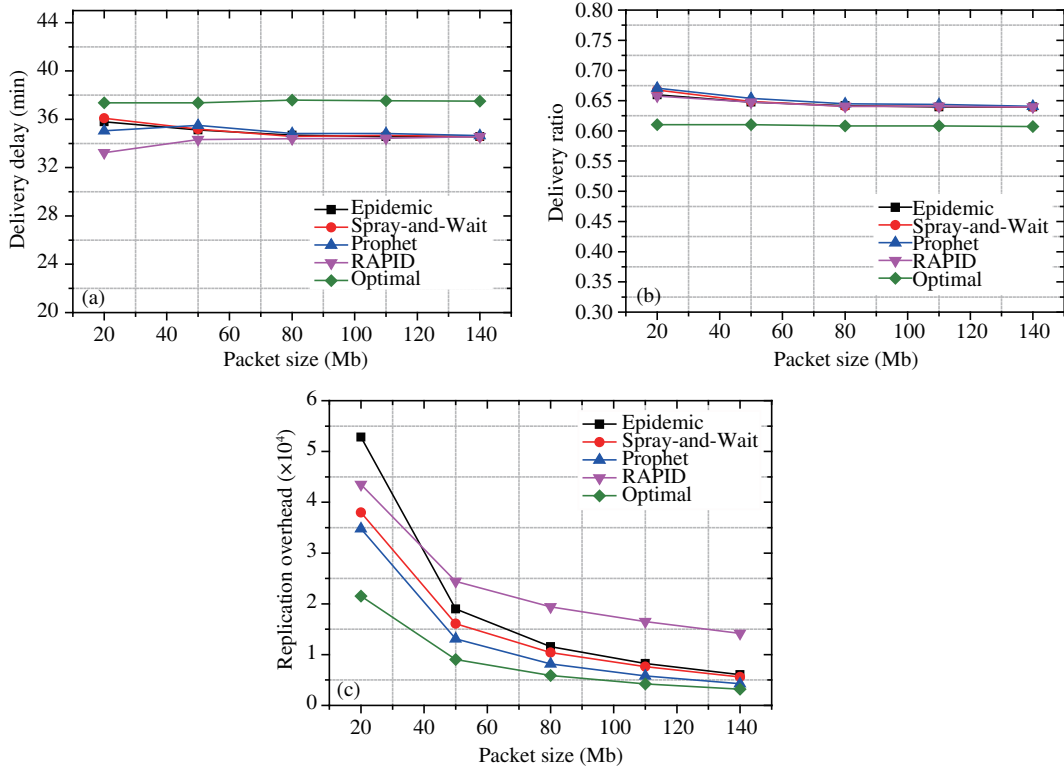


Figure 8 (Color online) Performance of data routing with different packet size. (a) Delivery delay; (b) delivery ratio; (c) replication overhead.

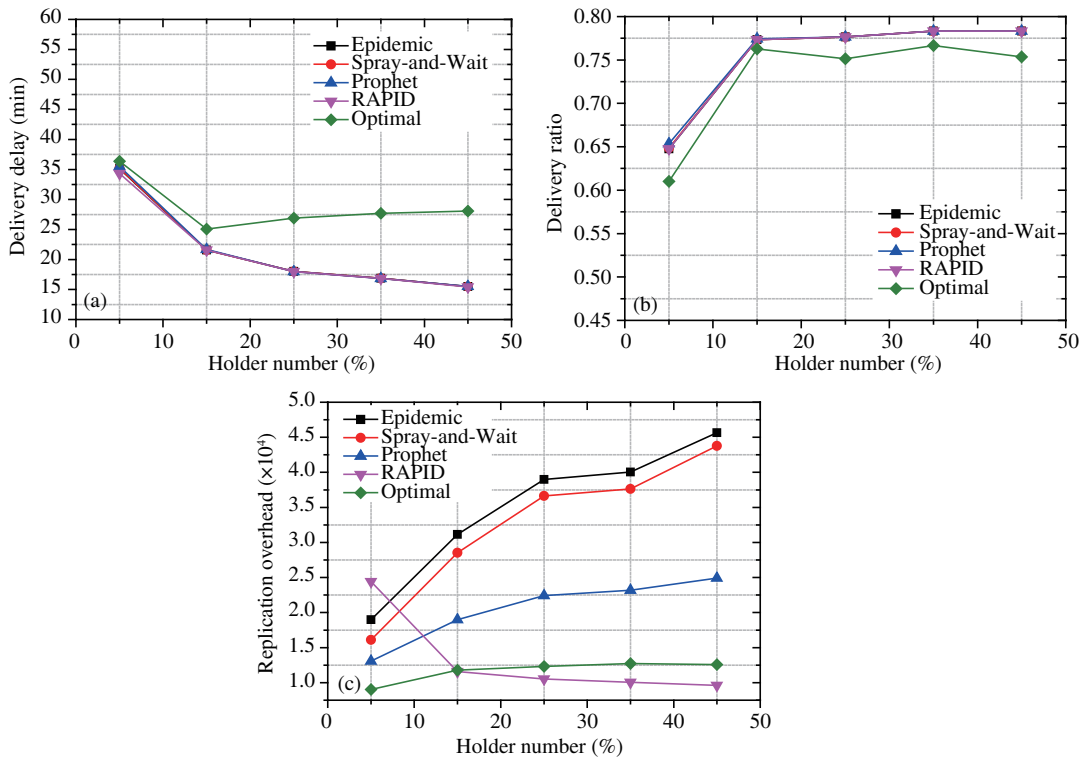


Figure 9 (Color online) Performance of data routing with different number of holders. (a) Delivery delay; (b) delivery ratio; (c) replication overhead.

of Epidemic, Spray-and-Wait, Prophet, RAPID as the curves nearly coincides. Surprisingly, the performance of Optimal degrades when percentage of holder number exceeds 15%. The reason behind this phenomenon is once a data request is generated, every holder has to respond by sending the requested packets. However, when holder number increases, such mechanism will produce tremendous packets appended with fixed routing paths, which leads to packet blocking at relay nodes.

Similar in Figure 9(b), the performances of all schemes except Optimal are exactly the same when percentage of holder number is above 15%. Besides, it brings little improvement of delivery ratio when holder number increases to some extent. Optimal yields lower delivery ratio than that of other schemes by 3.2% on average. Figure 9(c) shows that when holder number rises, the replication overhead of Epidemic and Spray-and-Wait increase sharply while Prophet and Optimal increase in moderate scale. The opposite trend of RAPID mainly results from the utility-based replication, which can be illustrated as if a packet is owned by many holders, replication can not improve marginal utility. Optimal yields smaller number of copies than that of Epidemic by 193%, Spray-and-Wait by 172%, Prophet by 73.6%, RAPID by 46.3%. Summarizing, in offloading scenario, it is impractical to ensure high density coverage of data items, most of them are distributed sparsely, which means Optimal is still applicable with its outstanding performance on replication overhead and tolerable gap respect to delivery delay and ratio.

6 Conclusion

In this paper, we propose an optimization model for routing strategies, which is fragmentation-based and applied to offloading scenario. The basic idea is to split the raw data into several packets initially, then create the model by formulating a fragmentation problem, aiming at maximizing the probability that data is successfully delivered before expiration. To make our model fundamental, we define specific mapping regulations to create two-tier solution space and use recursive formula to determine the probabilistic terms of objective goal. Moreover, a time-variant routing scheme called Optimal can be instantiated from our model through simplification of solution space, which is supported by uniform fragmentation and fine-grained path selection. Trace-driven simulations show that Optimal is appropriate for offloading case with outstanding performance in terms of replication overhead and acceptable routing capability.

Conflict of interest The authors declare that they have no conflict of interest.

Supporting information The supporting information is available online at info.scichina.com and link.springer.com. The supporting materials are published as submitted, without typesetting or editing. The responsibility for scientific accuracy and content remains entirely with the authors.

References

- 1 Cisco Visual Networking Index. Global Mobile Data Traffic Forecast Update, 2013–2018. White Paper, 2014
- 2 Zhuo X, Gao W, Cao G, et al. An incentive framework for cellular traffic offloading. *IEEE Trans Mobile Comput*, 2014, 13: 541–555
- 3 Li Y, Qian M, Jin D, et al. Multiple mobile data offloading through disruption tolerant networks. *IEEE Trans Mobile Comput*, 2013, 13: 1579–1596
- 4 Izumikawa H, Katto J. RoCNet: spatial mobile data offload with user-behavior prediction through delay tolerant networks. In: *IEEE Wireless Communications & Networking Conference, Shanghai, 2013*. 2196–2201
- 5 Dai Y, Cao G, Gao W, et al. Contact duration aware data replication in delay tolerant networks. In: *19th IEEE International Conference on Network Protocols, Vancouver, 2011*, 1416: 236–245
- 6 Li Z, Liu Y, Zhu H, et al. Coff: contact duration aware cellular traffic offloading over delay tolerant networks. *IEEE Trans Vehicular Tech*, 2014, 64: 5257–5268
- 7 Zhang X, Neglia G, Kurose J, et al. Benefits of network coding for unicast application in disruption-tolerant networks. *IEEE/ACM Trans Netw*, 2013, 21: 1407–1420
- 8 Pitkanen M, Keränen A, Ott J. Message fragmentation in opportunistic DTNs. In: *International Symposium on World of Wireless, Mobile and Multimedia Networks, Newport Beach, 2008*. 1–7
- 9 Ding L, Wu P, Wang H, et al. Lifetime maximization routing with network coding in wireless multihop networks. *Sci China Inf Sci*, 2013, 56: 022303

- 10 Ma Y, Jamalipour A. A cooperative cache-based content delivery framework for intermittently connected mobile ad hoc networks. *IEEE Trans Wirel Commun*, 2010, 9: 366–373
- 11 Masiero R, Neglia G. Distributed subgradient methods for delay tolerant networks. In: *Proceedings of IEEE INFOCOM*, Shanghai, 2011. 261–265
- 12 Picu A, Spyropoulos T. DTN-meteo: forecasting the performance of DTN protocols under heterogeneous mobility. *IEEE/ACM Trans Netw*, 2014, 23: 587–602
- 13 Lindgren A, Doria A, Schelén O. Probabilistic routing in intermittently connected networks. *Sigmobile Mobile Comput Commun Rev*, 2004, 7: 19–20
- 14 Balasubramanian A, Levine B N, Venkataramani A. Replication routing in DTNs: a resource allocation approach. *IEEE/ACM Trans Netw*, 2010, 18: 596–609
- 15 Elwhishi A, Ho P, Naik K, et al. Self-adaptive contention aware routing protocol for intermittently connected mobile networks. *IEEE Trans Parall Distr Syst*, 2013, 24: 1422–1435
- 16 Spyropoulos T, Psounis K, Raghavendra C S. Efficient routing in intermittently connected mobile networks: the single-copy case. *IEEE/ACM Trans Netw*, 2008, 16: 63–76
- 17 Spyropoulos T. Efficient routing in intermittently connected mobile networks: the multiple-copy case. *IEEE/ACM Trans Netw*, 2008, 16: 77–90
- 18 Abdelkader T, Naik K, Nayak A, et al. SGBR: a routing protocol for delay tolerant networks using social grouping. *IEEE Trans Parall Distr Syst*, 2013, 24: 2472–2481
- 19 Chen K, Shen H. Smart: utilizing distributed social map for lightweight routing in delay-tolerant networks. *IEEE/ACM Trans Netw*, 2014, 22: 1545–1558
- 20 Gao W, Li Q, Zhao B, et al. Social-aware multicast in disruption-tolerant networks. *IEEE/ACM Trans Netw*, 2012, 20: 1553–1566
- 21 Daly E, Haahr M. Social network analysis for information flow in disconnected delay-tolerant manets. *IEEE Trans Mobile Comput*, 2009, 8: 606–621
- 22 Hui P, Crowcroft J, Yoneki E. BUBBLE Rap: social-based forwarding in delay-tolerant networks. *IEEE Trans Mobile Comput*, 2011, 10: 1576–1589
- 23 Gao W, Cao G, Porta T L, et al. On exploiting transient social contact patterns for data forwarding in delay-tolerant networks. *IEEE Trans Mobile Comput*, 2013, 12: 151–165
- 24 Karagiannis T, Boudec J L, Vojnović M. Power law and exponential decay of intercontact times between mobile devices. *IEEE Trans Mobile Comput*, 2010, 9: 1377–1390
- 25 Gao W, Cao G, Iyengar A, et al. Cooperative caching for efficient data access in disruption tolerant networks. *IEEE Trans Mobile Comput*, 2013, 13: 611–625
- 26 Shaked M, Shanthikumar J. *Stochastic Orders and Their Applications*. New York: Academic Press, 1994
- 27 Tie X, Venkataramani A, Balasubramanian A. R3: robust replication routing in wireless networks with diverse connectivity characteristics. In: *Proceedings of the 17th Annual International Conference on Mobile Computing and Networking*. New York: ACM, 2011. 181–192
- 28 Chaintreau A, Hui P, Crowcroft J, et al. Impact of human mobility on opportunistic forwarding algorithms. *IEEE Trans Mobile Comput*, 2007, 6: 606–620